J Solid State Electrochem (2010) 14:115–121
DOI 10.1007/s10008-009-0796-3

ORIGINAL PAPER

# $SiO_2/TiO_2/Sb_2O_5$/graphite carbon ceramic conducting material: preparation, characterization, and its use as an electrochemical sensor

**Camila M. Maroneze · Rita C. S. Luz · Richard Landers · Yoshitaka Gushikem**

Received: 2 December 2008 / Revised: 23 January 2009 / Accepted: 26 January 2009 / Published online: 14 February 2009


**Abstract** $SiO_2/TiO_2$/graphite (STG) electrically conducting material, prepared by the sol–gel processing method, was used as substrate base for the chemical immobilization of Sb(V) by formation of the Ti–O–Sb linkage. The surface modified material, STGSb, was characterized by X-ray photoelectron spectroscopy and scanning electronic microscopy coupled to energy dispersive spectroscopy. The results showed the Sb(V) homogeneously dispersed on the STG matrix surface, with no phase segregation or isolated pure oxide domains. An electrode prepared with the STGSb material was used to adsorb the electroactive cationic dye meldola blue. The modified electrode, STGSb/MB, presented good performance toward electrocatalytic oxidation of the coenzyme β-NADH (nicotinamide adenine dinucleotide). The electrode was shown to be very stable and allowed the electrochemical detection of NADH at low electrode potential (−0.14 V), which is an interesting feature of the system since in this potential range it is possible to minimize surface fouling and electrode passivation. The support material (STGSb) has proven to have great potential to be applied in the construction of various new electrochemical sensors based on cationic dyes presenting redox properties.

**Keywords** $SiO_2/TiO_2/Sb_2O_5$/graphite composite material · Meldola blue · Electrocatalytic oxidation · NADH

C. M. Maroneze · R. C. S. Luz · Y. Gushikem (✉)
Instituto de Química, Universidade Estadual de Campinas,
P.O. Box 6154, 13084-971 Campinas, SP, Brazil
e-mail: gushikem@iqm.unicamp.br

R. Landers
Instituto de Física Gleb Wataghin,
Universidade Estadual de Campinas,
13084-971 Campinas, SP, Brazil

## Introduction

Porous mixed oxides like $SiO_2/M_xO_y$ ($M$=Ti(IV), Zr(IV), Sn(IV), Nb(V)) have been described in the literature as versatile materials to be applied in several areas [1–5], including electrochemistry [6–8]. This property results from the ability of these mixed oxides to react and immobilize on their surface acid species with ion exchange capacities such as phosphate groups attached onto $SiO_2/TiO_2$ and $SiO_2/ZrO_2$ composites [9, 10]. The resulting acidic system can be used to adsorb electroactive molecules by ion exchange reactions, and these solids have presented suitable features to be applied in the development of electrochemical sensors [11].

Antimony oxide, $Sb_2O_5$, is a well-known material having good Brφnsted acid properties, but its poor mechanical properties do not allow its direct application in electrochemical devices. One field in which $Sb_2O_5$ has been extensively studied is for the preparation of antimony-doped tin oxide anodes on titanium substrates ($Ti/SnO_2$–$Sb_2O_5$), which have shown good catalytic properties toward the electrochemical oxidation of organic contaminants, playing an important role in the disinfection of water, wastewater, and the treatment of industrial waste streams [12–15]. One possible alternative that makes $Sb_2O_5$ an interesting material to be applied in the development of new electrochemical sensors is the dispersion of $Sb_2O_5$ into rigid matrices [16, 17], i.e., the binary mixed oxides $SiO_2/M_xO_y$ cited above, which gives it the mechanical and chemical stability necessary to obtain good performance. This paper describes the surface modification of a conducting carbon ceramic composite material consisted of $SiO_2/TiO_2$/graphite [18], aiming to immobilize the $Sb_2O_5$ species on its surface. This material was then utilized in the adsorption of an electroactive cationic dye (meldola blue) and in the construction of an efficient carbon ceramic electrode for

NADH (β-nicotinamide adenine dinucleotide) electrochemical detection. NADH is an important molecule in many biochemical reactions acting as a coenzyme for a series of dehydrogenaze enzymes. Its direct determination on bare electrode surfaces occurs at high overpotential [19, 20], generally resulting in the rapid passivation and fouling of the electrode surface [21, 22]. Thus, there is a great need for a practical method to decrease the large overvoltage (≈1 V) observed in direct electrochemical oxidation of NADH at conventional electrodes. The proposed electrode is prepared without the use of organic binders and represents an alternative to the so-called carbon paste electrodes, specifically those ones prepared with non-conducting sol–gel materials. The development of a new electrode material as well as the adsorption of an electrochemical mediator, which promotes an indirect oxidation of NADH at low potential, is here proposed as a good alternative to overcome these problems.

## Experimental

### Surface modification of $SiO_2/TiO_2$/graphite

The $SiO_2/TiO_2$/graphite (STG) composite was prepared by the sol–gel processing method according to a procedure described elsewhere [18, 23].

About 10 g of STG presenting 55 wt.% $SiO_2$/16 wt.% $TiO_2$/29 wt.% graphite and a specific surface area of $S_{BET}$= 258 $m^2\ g^{-1}$ was immersed in 250 mL of an acidic aqueous solution (2.5 M HCl (Nuclear) of 0.5 M $SbCl_5$; 99%, Aldrich). The mixture was stirred at 333 K for 4 h. The solid was filtered, washed with 1.0 M HCl solution in order to avoid Sb(V) hydrolysis, and then washed with deionized water until the washing solution achieved a pH between 5 and 5.5. The sample obtained was designated as STGSb.

### Scanning electron microscopy

Secondary electron images were acquired in a JEOL JSM 6360LV scanning electron microscope, operating at 20 kV. Energy dispersive X-ray spectroscopy (EDS) was used for elemental mapping on a Noran System Six instrument. The sample was fixed onto double-faced carbon tape adhered to an aluminum support and carbon-coated in a Bal-Tec MD20 instrument.

### X-ray photoelectron spectroscopy

The X-ray photoelectron (XPS) spectra of the sample were obtained by using an aluminum anode (AlKα=1,486.1 eV) at a pressure of $2.63\times10^{-5}$ Pa on a McPherson ESCA-36 spectrometer. The binding energies were calibrated against the Si2p level (103.5 eV) [24].

### Preparation of the working electrode/electrochemical measurements

The working electrode was prepared by pressing 30 mg of STGSb under a pressure of 5 tons. The resulting self-supported disk (3 mm radius) was glued to the end of a glass tube. A copper wire linked to the disk by graphite powder inserted inside the tube made the electrical contact. The immobilization of the electroactive dye was carried out by immersing the working electrode into a $1.0\times10^{-4}$ M aqueous solution of meldola blue ($MB^+$) for half an hour. Next, the electrode was washed with bidistilled water.

The electrochemical measurements were carried out on an Autolab PGSTAT 20 potentiostat-galvanostat apparatus, using a classical three-electrode cell. A saturated calomel electrode (SCE) was used as the reference electrode, a platinum foil as the auxiliary electrode, and a pressed disk of STGSb as working electrode. All measurements were carried out in 0.1 M phosphate buffer solution at pH7.5.

## Results and discussion

### Scanning electron microscopy and EDS mapping

Figure 1 shows the scanning electron microscopic images of STGSb and the energy dispersive scanning images of Si, Ti, and Sb mapping.

The scanning electron microscopy (SEM) micrographs of STGSb presented in Fig. 1a–c, within the magnification used, show that there are no distinguishable separated phases. The EDS images also show that the components are homogeneously dispersed in the sample with no detectable agglomeration of segregated metal oxide particles.

### X-ray photoelectron spectroscopy

The XPS spectra for STGSb sample are presented in Fig. 2.

The binding energies of Sb 4d, Sb $3d_{3/2}$, and Sb 4p in the STGSb confirm the incorporation of Sb(V) on the STG matrix. The energy values are in agreement with those for pure bulk $Sb_2O_5$ and indicate the presence of this species on the surface.

The incorporation of Sb(V) on the matrix surface can be described by the reaction between the surface ≡Ti–OH groups and the acid sites of $Sb(OH)_5$, forming the linkage $(\equiv Ti–O)_nSb(OH)_{5-n}$ according to the reaction [16, 25]:

$$n\mathrm{GSiO_2/TiOH} + \mathrm{Sb(OH)_5} \rightarrow (\mathrm{GSiO_2/TiO})_n\mathrm{Sb(OH)_{5-n}} + n\mathrm{H_2O} \quad (1)$$

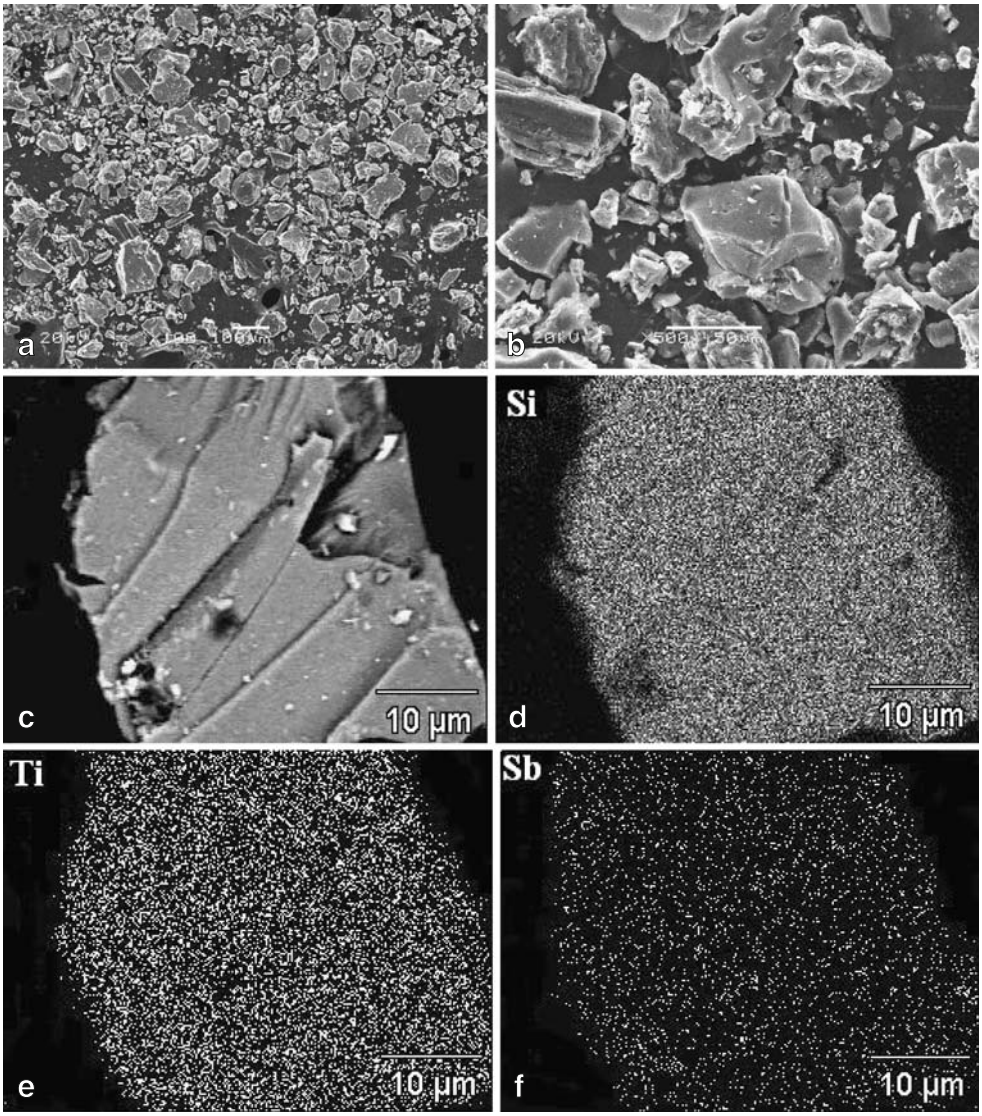


**Fig. 1** Scanning electron microscopic images of STGSb in **a**, **b**, and **c** and the corresponding EDS images for **d** Si mapping, **e** Ti mapping, and **f** Sb mapping

It must be remembered that Sb(V) does not react with silanol (≡Si–OH) groups in aqueous acid solutions, except when $SiO_2$, dried under vacuum, is reacted with $SbCl_5$ in an aprotic solvent under a water free atmosphere [26, 27]. It has been observed that Si–O–Sb bond formed under such conditions is broken in strong acid solution, and the metal Sb(V) is released to the solution phase.

The BE values for $Ti2p_{3/2}$ and $Ti2p_{1/2}$ in STGSb are shifted upward when compared to pure $TiO_2$ phase. These dislocations to higher energies confirm our hypothesis and are related to the interaction of Ti with Sb. The linkage Ti–O–Sb polarizes this bonding, decreasing the electron density on the Ti atom since the Sb atom is more electronegative so that the Ti2p BE is shifted to higher energy values.

## Electrochemical measurements

After the working electrode preparation, the adsorption of the electroactive cationic dye meldola blue ($MB^+$) was carried out by immersing the STGSb electrode into an aqueous solution of $MB^+$. The adsorption of the electroactive species occurs by an ion exchange reaction, as described below:

$$\equiv \mathrm{SbOH} + \mathrm{MB}^+ \rightarrow \equiv \mathrm{SBO}^-\mathrm{MB}^+ + \mathrm{H}^+ \quad (2)$$

where SbOH stands for hydrated antimony(V) dispersed on the STG matrix. The modified electrode will hereafter be designated as STGSb/MB.

Figure 3 shows the cyclic voltammograms of STGSb (curve (a)) and STGSb/MB (curve (b)), obtained in 0.1 M phosphate buffer solution (pH7.5) at a scan rate of 20 mV $s^{-1}$.

In Fig. 3 (a), the electrode STGP showed no peak current in the potential range between −0.4 and 0.2 V, indicating no redox process at the electrode surface. In contrast, in Fig. 3 (b) for the modified STGSb/MB electrode, a well-defined redox couple $E_{pa}$=−0.1 and $E_{pc}$=−0.21 V are observed. The corresponding anodic and cathodic peak current intensities, $i_{pa}$ and $i_{pc}$, were shown to remain constant after several

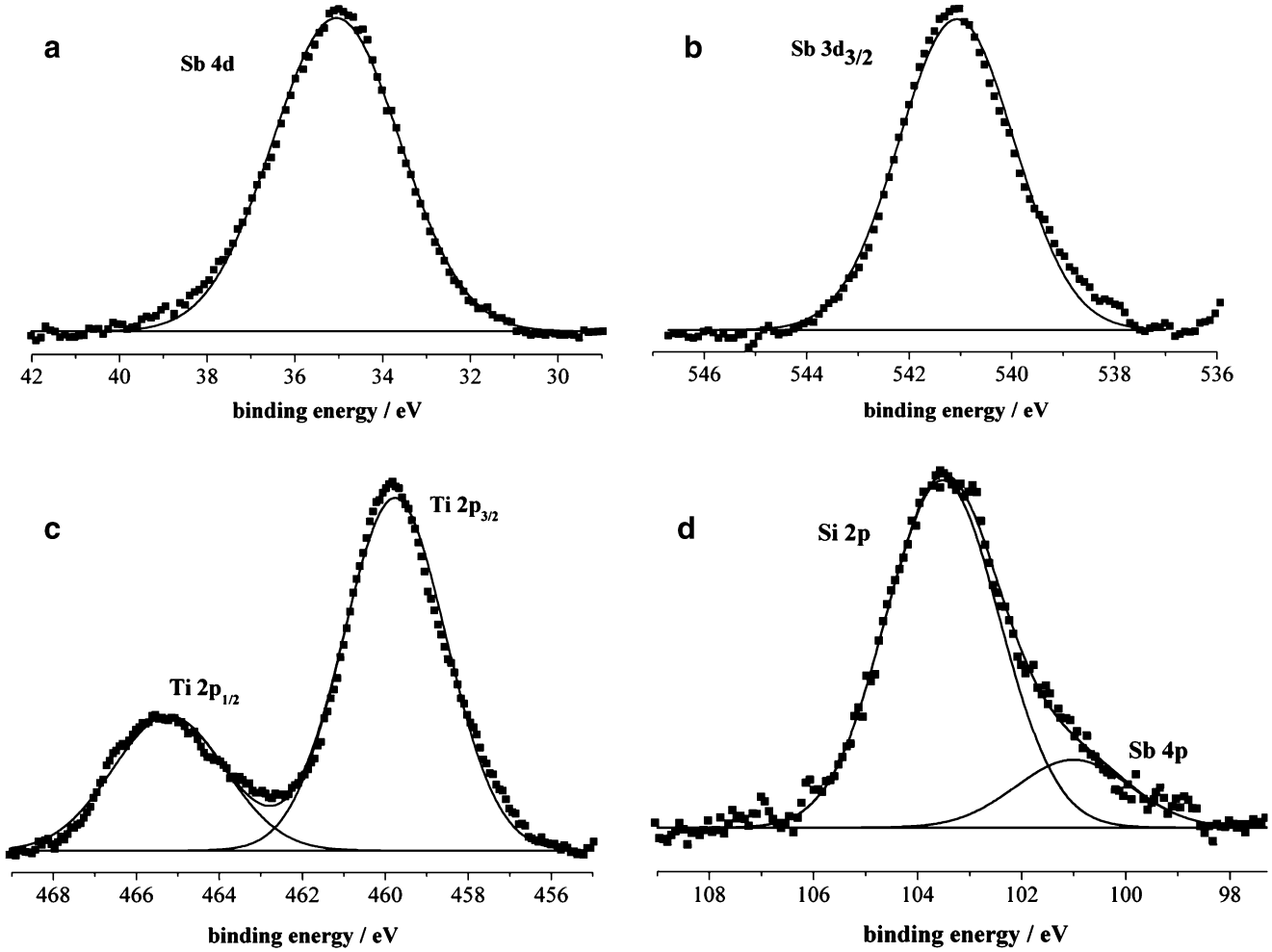


**Fig. 2** XPS spectra for STGSb: **a** Sb 4d, **b** Sb $3d_{3/2}$, **c** Ti 2p, and **d** Si 2p and Sb 4p

consecutive scanning cycles, indicating that the dye is strongly retained on the matrix surface, presumably confined inside the matrix pores since, on the time-scale of the experiment, no release of the dye to the solution phase is detected.

The peak current for a strongly adsorbed electroactive species is given by Eq. 3 [28–31]:

$$I_p = \frac{n^2F^2A\Gamma\nu}{4RT} \quad (3)$$

where $A$ is the geometrical surface area, $\nu$ is the scan rate (V $s^{-1}$), $\Gamma$ is the surface concentration of the electroactive species, and the other symbols have their usual meanings.

The adsorptive or surface confined redox process behavior of meldola blue was confirmed by registering cyclic voltammograms at various potential scan rates from 10 up to 100 mV $s^{-1}$ (Fig. 4a).

The linear correlation of the $I_p$ with the scan rates, $v$, clearly shows a redox process of strongly adsorbed electroactive species on the electrode surface (Fig. 4b). From the

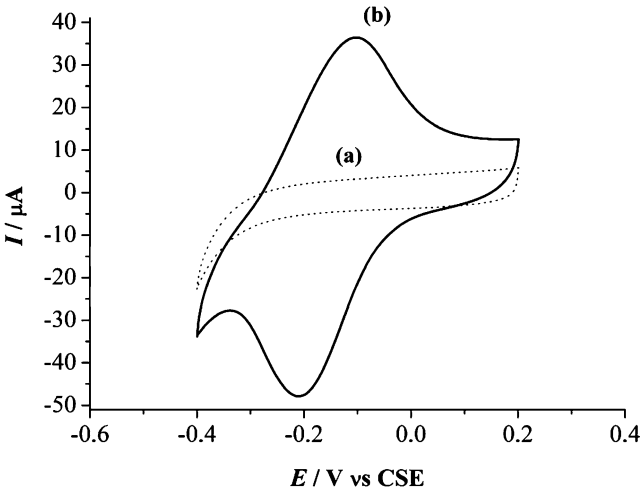


**Fig. 3** Cyclic voltamogramms of the *(a)* STGP and *(b)* STGP/MB electrodes. Measurements carried out in 0.1 mM phosphate buffer solution (pH 7.5). Scan rate: 20 mV $s^{-1}$

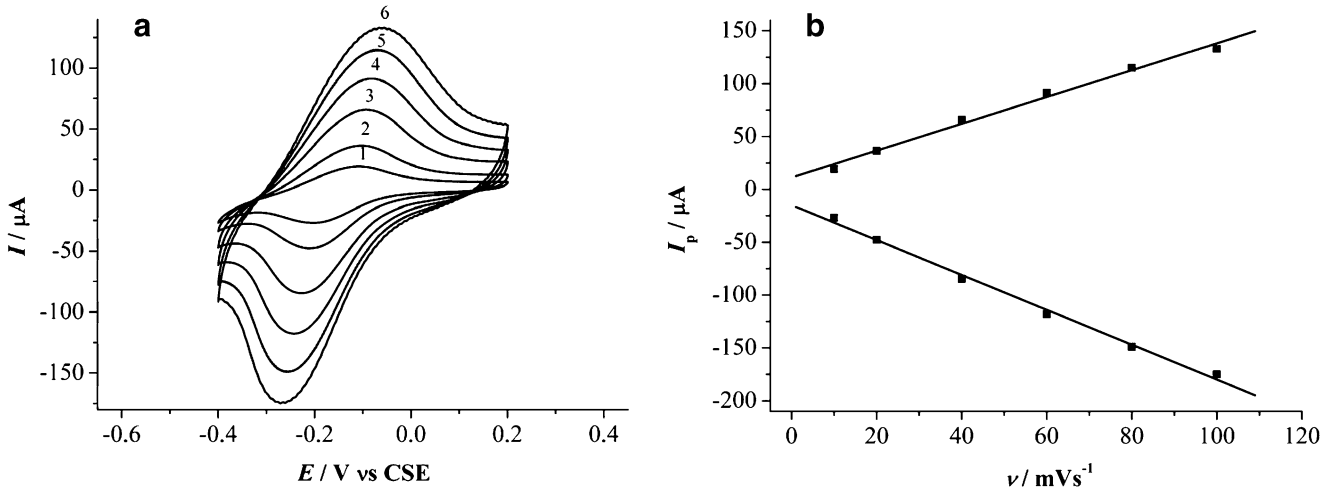


**Fig. 4** **a** Cyclic voltamogramms of the STGSb/MB electrode in 0.1 M phosphate buffer solution (pH7.5) at potential scan rates of (*1*) 10, (*2*) 20, (*3*) 40, (*4*) 60, (*5*) 80, and (*6*) 100 mV s$^{-1}$; **b** plot of $I_p - \nu$ obtained from **a**

slope of the plot of $I_{pa}$ vs scan rate, the surface electroactive species concentration was estimated, giving a value $\Gamma = 1.2\times10^{-9}$mol cm$^{-2}$ for an electrode with a geometric surface area $A$=0.28 cm$^2$.

The solution pH dependence on the electrochemical behavior of meldola blue on the STGSb/MB electrode was studied in different buffer solutions (pH5.0–7.5) in the absence of NADH. A pair of well-defined redox peaks with nearly equal currents, and strong pH dependence was obtained for adsorbed meldola blue at the different pH values. Both reduction and oxidation peak potentials of the $MB^+$/MBH redox couple shifted negatively with an increase in pH. The midpoint potential of the surface redox couple, taken as the average of anodic and cathodic peak potentials, $E_m = (E_{pa} + E_{pc})/2$, was linearly pH dependent between 5.0 and 7.5, with a slope of 0.20 V per unit of pH (data not shown) indicating that the electrode reaction involves one proton and two electrons [32].

## Electrocatalytic oxidation of NADH

The electrocatalytic activity of meldola blue adsorbed on STGSb/MB electrode was tested for NADH oxidation. Figure 5 shows the cyclic voltammograms of STGSb and STGSb/MB electrodes in the absence and presence of 10 mM NADH.

Figure 5a shows that no peak current is present for the STGSb electrode when cycling the potential between −0.35 and 0.05 V in the absence (curve 1) and presence (curve 2) of NADH at 10 mM in 0.1 M phosphate buffer solution

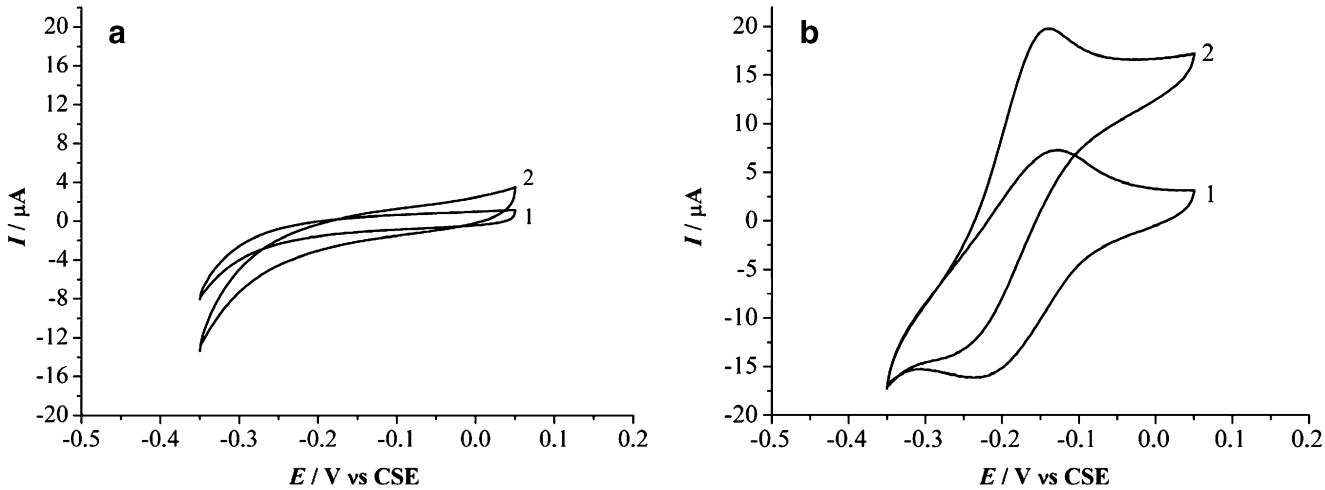


**Fig. 5** Cyclic voltammograms for **a** STGSb electrode in the absence (*curve 1*) and the presence of NADH (10 mM; *curve 2*), **b** STGSb/MB electrode in the absence (*curve 1*) and the presence of NADH (10 mM; *curve 2*)

(pH7.5). However, when the same experiment was carried out with the modified electrode (STGSb/MB), there is a dramatic enhancement of the anodic peak current and the cathodic peak current disappears completely (Fig. 5a, curve 2), which is very characteristic of an electrocatalytic oxidation process. The anodic peak potential for oxidation of NADH at the STGSb/MB electrode is about −0.14 V (Fig. 5b, curve 2), while at an unmodified STGSb electrode under identical conditions, it is more than 1 V and exhibits a peak current (Fig. 5a, curve 2) lower than that observed with a STGSb/MB electrode.

The low potential applied to carry out this analysis is an important feature of our system, placed in a potential range between 0 and≈−0.2 V where contributions to the response from easily oxidisable species are negligible, where molecular oxygen is not electrochemically reduced, and where the potential of zero charge is found for most electrode materials, resulting in low background current and noise [33].

The plot of the peak current $I_p$ vs the square root of the potential scan rate $\nu_{,}^{1/2}$ obtained from voltammograms of the STGSb/MB electrode in 0.1 M phosphate buffer solution (pH7.5) containing 10 mM NADH, shows that the oxidation currents for NADH increase linearly with the square root of the scan rate in the range studied. These results show that the overall electrochemical oxidation of NADH at this electrode might be controlled by the diffusion of NADH from solution to the redox sites of STGSb/MB electrode.

## Characterization of the electrode

In order to obtain the analytical curve for the electrode, chronoamperograms for NADH oxidation were carried out at several NADH concentrations in 0.1 M phosphate buffer at pH7.5 (applied potential −0.14 V). The proposed sensor shows a large linear response range from 0.0009 to 7.29 M (Fig. 6), which can be expressed according to the following equation:

$$I_p/\mu A = 0.15(\pm 0.03) + 0.943(\pm 10.6)[\mathrm{NADH}]/(\mathrm{mM}) \quad (4)$$

with a correlation coefficient of 0.999. A detection limit of 0.003 mM was determined using a $3\sigma$/slope ratio, where $\sigma$ is the standard deviation calculated from the ten background current values (blank measurements), determined according to IUPAC recommendations [34].

The stability of the STGSb/MB electrode was checked in the presence of 10 mM NADH by performing successive voltammetric measurements in 0.1 M phosphate buffer solution (pH7.5). After 200 voltammetric measurements, no change was observed in the response of the modified electrode.

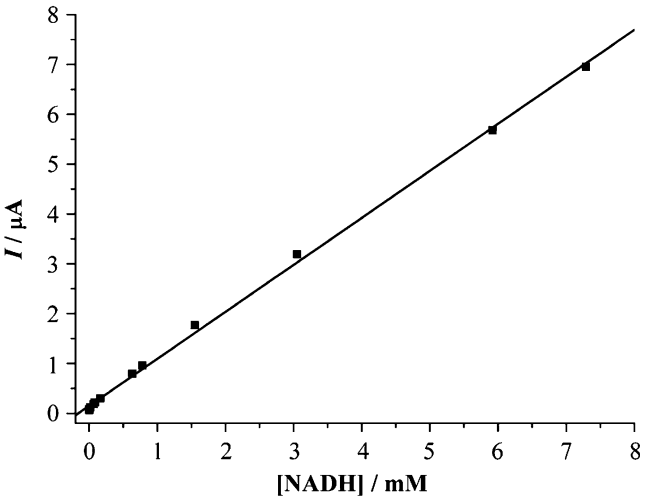


**Fig. 6** Calibration plot for the electro-oxidation of NADH obtained in phosphate buffer solution at pH7.5 for the concentrations: 0.0009, 0.0039, 0.009, 0.02, 0.07, 0.08, 0.16, 0.63, 0.78, 1.55, 3.05, 5.92, and 7.29 mM. $E_{appl}$=−0.14 V vs SCE

The STGSb/MB electrode presented good repeatability for the NADH determination, tested using cyclic voltammetry. The relative standard deviation for ten determinations of 10 mM NADH was 1.49%. These results indicate that the STGSb/MB electrode has good stability and repeatability, probably due to the ability of STGSb to fix meldola blue on the electrode surface in a stable and reproducible way.

When compared to the $SiO_2/TiO_2$/phosphate/graphite system (STGP/MB) [18], the $SiO_2/TiO_2/Sb_2O_5$/graphite (STGSb/MB) carbon ceramic electrode has showed a lower detection limit, higher sensitivity, and a wider linear response range for NADH determination. This behavior can be related to a more effective interaction between the meldola blue mediator and the stronger acid sites of antimonate than those of phosphate species, which results in higher affinity between the catalist and the analite, and consequently higher efficiency in the electron transfer processes. This possibility is also evidenced by the influence of the solution pH on the midpoint potential ($E_m$) of the surface redox couple $MB^+$/MBH. In both cases, a linear correlation between $E_m$ and pH is observed, but with distinct slopes. A lower dependence was noted for the STGSb/MB system, which probably means that the electroactive mediator is adsorbed on surface groups with higher acidity and more strongly held by electrostatic interactions compared to STGP/MB [35].

## Conclusions

Chemical modification of a conducting STG composite material was successfully carried out by immobilizing Sb

(V) on its surface through reaction with≡Ti–OH and formation of the Ti–O–Sb bond. The resulting material, STGSb, was analyzed by X-ray photoelectron spectroscopy, which showed the incorporation of Sb(V), probably through the formation of a titanium antimonate phase. SEM images coupled to surface element mapping (EDS) indicate that there is no segregation phase and that the components are homogeneously dispersed in the matrix. The STGSb material presented good acidic properties, which made it possible to adsorb an electroactive cationic dye (meldola blue) onto STGSb electrodes, resulting in a system with high electrocatalytic activity towards NADH oxidation, probably due to low resistance to charge transfer between the STGSb/MB and NADH. This work has demonstrated that the STGSb electrode is a robust and stable material showing to having good potential for the construction of new electrochemical sensors based on cationic dyes that present redox properties, which can easily be immobilized on the matrix surface by a simple ion exchange reaction.

**Acknowledgments** C.M.M is indebted to FAPESP (São Paulo State Research Support Foundation) for a PhD fellowship and YG is indebted for financial support (grant 00/11103-5). The authors are also indebted to the CNPq (National Research Council) for research grants and Prof. C.H. Collins for manuscript revision.

## References

1. Frenzer G, Maier WF (2006) Annu Rev Mater Res 36:281. doi:10.1146/annurev.matsci.36.032905.092408
2. Davis RJ, Liu ZF (1997) Chem Mater 9:2311. doi:10.1021/cm970314u
3. Miller JB, Ko EI (1996) J Catal 159:58. doi:10.1006/jcat.1996.0064
4. Canevari TC, Arguello J, Francisco MSP, Gushikem Y (2007) J Electroanal Chem 609:61. doi:10.1016/j.jelechem.2007.06.006
5. Ichikuni N, Shirai M, Iwasawa Y (1996) Catal Today 28:49. doi:10.1016/0920-5861(95)00228-6
6. Walcarius A, Mandler D, Cox JA, Collinson M, Lev O (2005) J Mater Chem 15:3663. doi:10.1039/b504839g
7. Walcarius A (2001) Chem Mater 13:3351. doi:10.1021/cm0110167
8. Lunsford SK, Choi H, Stinson J, Yeary A, Dionysiou DD (2007) Talanta 73:172. doi:10.1016/j.talanta.2007.03.002
9. Alfaya AAS, Gushikem Y, Castro SC (1998) Chem Mater 10:909. doi:10.1021/cm970679e
10. Alfaya AAS, Gushikem Y, Castro SC (2000) Microporous Mesoporous Mater 39:57. doi:10.1016/S1387-1811(00)00176-1
11. Marafon E, Kubota LT, Gushikem Y (2009) J Solid State Electrochem 13:377. doi:10.1007/s10008-008-0564-9
12. Watts RJ, Wyeth MS, Finn DD, Teel AL (2008) J Appl Electrochem 38:31. doi:10.1007/s10800-007-9391-4
13. Ding H, Feng Y, Liu J (2007) Mater Lett 61:4920. doi:10.1016/j.matlet.2007.03.073
14. Baker PGL, Sanderson RD, Crouch AM (2007) Thin Solid Films 515:6691. doi:10.1016/j.tsf.2007.01.042
15. Chen X, Gao F, Chen G (2005) J Appl Electrochem 35:185. doi:10.1007/s10800-004-6068-0
16. Castellani AM, Gonçalves JE, Gushikem Y (2001) Electroanalysis 13:1165
17. Zaitseva G, Gushikem Y, Ribeiro ES, Rosatto SS (2002) Electrochim Acta 47:1469. doi:10.1016/S0013-4686(01)00870-2
18. Maroneze CM, Arenas LT, Luz RCS, Benvenutti EV, Landers R, Gushikem Y (2008) Electrochim Acta 53:4167. doi:10.1016/j.electacta.2007.12.072
19. Moiroux J, Elving PJ (1978) Anal Chem 50:1056. doi:10.1021/ac50030a015
20. Jaegfeldt H (1980) J Electroanal Chem 110:295. doi:10.1016/S0022-0728(80)80381-0
21. Wang J, Anges L, Martinez T (1992) Bioelectrochem Bioenerg 29:215. doi:10.1016/0302-4598(92)80069-S
22. Musameh M, Wang J, Merkoci A, Lin Y (2002) Electrochem Commun 4:743. doi:10.1016/S1388-2481(02)00451-4
23. Gushikem Y, Benvenutti EV, Ribeiro ES (2003) "Silica-titania-graphite electrical conducting material obtained by the sol-gel processing method", Brazilian Patent, INPI-PI 0303303-1
24. Moulder JF, Stickle WF, Sobol PE, Bomben KD (2002) Handbook of X-ray photoelectron spectroscopy. Perkin-Elmer, Eden Prairie, MN
25. Gonçalves JE, Gushikem Y, Castro SC (1999) J Non-Cryst Solids 260:125. doi:10.1016/S0022-3093(99)00553-0
26. Benvenutti EV, Gushikem Y, Vasquez A, Castro SC, Zaldivar GAP (1991) J Chem Soc Chem Commun 19:1325. doi:10.1039/c39910001325
27. Benvenutti EV, Gushikem Y, Davanzo CU, Castro SC, Torriani IL (1992) J Chem Soc Faraday Trans 88:3193. doi:10.1039/ft9928803193
28. Bard AJ, Faulkner LR (2001) Electrochemical methods. Fundamentals and applications, 2nd edn. Wiley, New York
29. Laviron E (1979) J Electroanal Chem 101:19. doi:10.1016/S0022-0728(79)80075-3
30. Honeychurch MJ, Rechnitz GA (1998) Electroanalysis 10:285. doi:10.1002/(SICI)1521-4109(199804)10:5<285::AID-ELAN285>.0.CO;2-B
31. Manisankar P, Gomathi A, Velayutham D (2005) J Solid State Electrochem 9:601. doi:10.1007/s10008-004-0610-1
32. Zhu L, Zhai J, Yang R, Tian C, Guo L (2007) Biosens Bioelectron 22:2768. doi:10.1016/j.bios.2006.12.027
33. Gorton L, Domínguez E (2002) Rev Mol Biotechnol 82:371. doi:10.1016/S1389-0352(01)00053-8
34. Analytical Methods Committee (1987) Analyst (Lond) 112:199. doi:10.1039/an9871200199
35. Pessoa CA, Gushikem Y, Kubota LT, Gorton L (1997) J Electroanal Chem 431:23. doi:10.1016/S0022-0728(97)00168-X